Available online at website: https://journal.bcrec.id/index.php/bcrec

Bulletin of Chemical Reaction Engineering & Catalysis, 21 (1) 2026, 96-111

Original Research Article

Green-Modified Ni/Al LDH with *Camellia sinensis* Bioactives: A Sustainable Strategy for Ceftriaxone Removal

Amri Amri[1,2], Najma Annuria Fithri[3], Muhammad Said[4], Aldes Lesbani[2,5]*

[1]*Doctoral Program of Environmental Science, Postgraduate Program, Universitas Sriwijaya, Palembang, 30139, Indonesia.*
[2]*Research Center of Inorganic Materials and Coordination Complexes, Universitas Sriwijaya, Palembang, 30139, Indonesia.*
[3]*Department of Pharmacy, Faculty of Mathematics and Natural Sciences, Universitas Sriwijaya, Ogan ilir, 30862, Indonesia.*
[4]*Department of Chemical Engineering, Faculty of Engineering, Universitas Sriwijaya, Ogan ilir, 30862, Indonesia.*
[5]*Magister Program of Materials Science, Graduate School Universitas Sriwijaya, Palembang, 30139, Indonesia.*

Received: 14th October 2025; Revised: 5th December 2025; Accepted: 6th December 2025
Available online: 15th December 2025; Published regularly: April 2026

Abstract

Ceftriaxone (CEF) is a β-lactam antibiotic widely used in the medical field to treat various bacterial infections in both humans and animals. The high usage of CEF has the potential to cause environmental pollution and antimicrobial resistance, necessitating effective treatment methods. In this study, the adsorption method is proposed using Ni/Al layered double hydroxide (LDH) and *Camellia sinensis* extract-modified material (Ni/Al-CSe) as a sustainable bio-modification approach. The results show the optimal adsorption pH for Ni/Al LDH is 3 and for Ni/Al-CSe is 5, with the adsorption isotherms following the Freundlich model and the kinetics conforming to pseudo-first order (PFO). The maximum adsorption capacity (Q_m) significantly increased from 28.818 mg.g^{-1} (Ni/Al LDH) to 111.111 mg.g^{-1} (Ni/Al-CSe). Thermodynamic analysis revealed that adsorption on both materials proceeds spontaneously, while the consistently more negative ΔG values and predominantly exothermic behavior of Ni/Al-CSe confirm its superior thermodynamic favorability associated with more specific surface interactions. Regeneration tests up to four cycles showed that Ni/Al-CSe was more stable than Ni/Al LDH. Overall, modifying Ni/Al LDH with *Camellia sinensis* extract was proven to enhance adsorption capacity, spontaneity, and stability, providing an effective and environmentally friendly solution for antibiotic treatment.

Keywords: Ni/Al LDH; *Camellia sinensis*; Composite; Adsorption; Ceftriaxone

How to Cite: Amri, A., Fithri, N. A., Said, M., Lesbani, A. (2026). Green-Modified Ni/Al LDH with *Camellia sinensis* Bioactives: A Sustainable Strategy for Ceftriaxone Removal. *Bulletin of Chemical Reaction Engineering & Catalysis*, 21 (1), 96-111. (doi: 10.9767/bcrec.20513)

Permalink/DOI: https://doi.org/10.9767/bcrec.20513

1. Introduction

In recent decades, the use of pharmaceutical drugs has increased rapidly worldwide. More than 200,000 tons of medication are consumed annually to treat various human diseases, including steroid hormones, anti-inflammatory drugs, and antibiotics. It is known that between 30 and 90% of drug compounds, both in their parent form and as active metabolites, can be excreted thru urine and feces. As a result, these compounds can enter the aquatic environment without undergoing complete degradation [1,2]. Among various pharmaceutical groups, antibiotics are one of the most frequently detected wastes in water bodies. This is due to the disposal of antibiotics in their original form or as metabolites thru domestic waste, the disposal of expired drugs, and the activities of the pharmaceutical industry [3]. Therefore,

* Corresponding Author.
Email: aldeslesbani@pps.unsri.ac.id (A. Lesbani)

antibiotics show an increase in the accumulation and persistence of this substance in the environment. Additionally, the large-scale consumption of antibiotics, by both humans and animals, is further exacerbating the environmental burden, as most residues are disposed of without adequate treatment processes [4]. The excessive and inappropriate use of antibiotics has resulted in antibiotic-resistant bacteria and resistance genes, which have been found in drinking water, posing a significant threat to human health [5].

Ceftriaxone sodium (CEF) is a third-generation semi-synthetic antibiotic from the ß-lactam cephalosporin group [6–8]. Due to its resistance to the ß-lactamase enzyme, CEF is widely used in the medical world to treat various bacterial infections in humans and animals [9]. Because of its high usage, some of this chemical residue remains in the body and is eventually released into water thru excretion, household waste, and pharmaceutical industrial activities [7,9]. Its presence in the environment poses a significant problem because CEF compounds can affect microorganisms, plants, aquatic animals, and even human health by disrupting the ecosystem balance, even at low concentrations [10,11].

To address antibiotic pollution in the environment, including CEF, various methods have been developed, including physical, chemical, and biological processes. Membrane filtration, nanofiltration, reverse osmosis, ion exchange, activated sludge systems, Fenton-like reactions, ozonation, photolysis, and magnetic ion exchange resins are some commonly used techniques [9,12,13]. However, most of these methods have limitations despite being effective in certain situations. Conversely, the adsorption method has emerged as one of the most promising approaches in wastewater treatment due to its many advantages, including simplicity, low operating costs, the absence of hazardous byproducts, and high effectiveness in removing various contaminants, including antibiotics [12,14–16].

The selection of adsorbent material is a crucial factor in the CEF adsorption process, as the material's physicochemical properties influence the efficiency of pollutant removal [17]. One material that has received significant attention is layered double hydroxide (LDH), which is a group of solids with a brucite-like structure and the general formula $[M^{II}_{(1-x)}M^{III}_x(OH)_2]^{x+} \cdot (A^{n-})_{(x/n)} \cdot yH_2O$, where M^{II} and M^{III} are divalent cations (e.g., Mg^{2+}, Zn^{2+}, Ni^{2+}, Ca^{2+}, Fe^{2+}) and trivalent cations (such as: Al^{3+}, Fe^{3+}, Cr^{3+}, Ga^{3+}), while A^{n-} is an exchangeable anion in the interlayer space [18–21]. The layered structure gives LDH high anion exchange capacity, large surface area, good thermal stability, and ease of synthesis at relatively low cost, making this material widely used in various applications, including catalysis, electrochemistry, and contaminant removal in water thru adsorption [19,22].

Despite its various advantages, the use of pure LDH still faces some limitations. This material tends to agglomerate in aqueous environments, thus reducing the active surface area available for interaction with pollutants [23]. Additionally, pure LDH is reported to have low mechanical stability and difficulty in regeneration, which limits its effectiveness in repeated applications [24,25]. These limitations have prompted many researchers to develop composite-based LDH with the addition of supporting materials or modification using natural compounds, aiming to improve stability, prevent agglomeration, and enhance adsorption performance [26].

Various previous studies have shown that the creation of LDH-based composites with the addition of other materials can significantly improve adsorption performance. For example, the ZnCr-LDH/Spirogyra algae composite showed a significantly higher adsorption capacity for Direct Yellow compared to pure LDH, with the Qm value increasing from 22.727 mg/g for ZnCr-LDH to 48.780 mg/g for ZnCr-LDH/ Spirogyra algae, while maintaining a removal efficiency of 56.37% after five cycles of use [27]. The Ni/Al-LDH composite with magnetic humic acid (Ni/Al-MAH) also proved to increase the adsorption capacity from 68.966 mg/g for pure LDH to 178.571 mg/g, indicating synergy between LDH and the magnetic organic material [28]. Another study reported that red mud/LDH nanocomposites are effective for the adsorption of the antibiotic sulfamethoxazole, with good regeneration ability up to six cycles without significant capacity reduction [29].

Additionally, the utilization of natural material extracts as a modification component also shows promising potential. For example, MgAl-LDH composites with Hylocereus costaricensis extract were reported to be reusable for up to three cycles without significant reduction in adsorption performance [30]. Similarly, NiFe-LDH composites with gambir leaf extract were able to be reused for up to five cycles with stable adsorption capacity [31]. The Zn/Al-LDH composite modified with thyme extract showed a maximum adsorption capacity (Q_m) of 49.751 mg/g for methylene blue [32]. Biological extract of Cynomorium coccineum has been used to synthesize copper nanoparticles with copper sulfate precursor, resulting in an adsorption capacity (Q_m) of 64 mg/g for methylene blue [33]. Additionally, magnetite nanoparticles (Fe_3O_4) produced by green synthesis using Moringa

oleifera extract were reported to remove the antibiotic levofloxacin with an adsorption capacity of 22.47 mg/g [34]. These results confirm that integrating LDH with biological materials and natural extracts not only enhances adsorption capacity but also improves regeneration properties and the sustainability of its use.

Although showing potential, the research still has limitations, including the fact that studies with thyme and Cynomorium coccineum extract were only tested on simple pollutants like methylene blue, while the use of Moringa oleifera extract still has low capacity against antibiotics. In this context, green tea leaf extract (*Camellia sinensis*) becomes an interesting modification candidate because it contains bioactive compounds such as polyphenols and flavonoids rich in hydroxyl groups, thus potentially enhancing the interaction between the composite material and antibiotic molecules [35,36]. The presence of hydroxyl and aromatic groups in these bioactive compounds allows for strong interactions with the LDH surface, thereby enhancing the adsorption capacity and selectivity of the composite material toward complex organic pollutants such as antibiotics [37]. Thus, the utilization of green tea leaf extract as an LDH modification agent is considered an innovative and environmentally friendly approach to enhance the performance of adsorbent materials.

Based on this background, this study aims to synthesize and evaluate the performance of Ni/Al layered double hydroxide (LDH) and its composite modified with green tea leaf extract (*Camellia sinensis*), namely Ni/Al-CSe, in the adsorption process of the antibiotic CEF from aqueous solutions. This study includes characterization of material surface structure and properties, evaluation of adsorption capacity, and regeneration tests to assess its sustainability. With this approach, it is hoped that composite materials will be obtained that are not only effective in removing antibiotics, but also support environmentally friendly pharmaceutical waste treatment strategies.

2. Materials and Method

2.1. Chemicals and Instrumentation

Green tea leaves (*Camellia sinensis*) are commercially obtained from the Mount Dempo area, South Sumatra, Indonesia. Chemicals of analytical purity were used in this study, namely nickel nitrate hexahydrate ($Ni(NO_3)_2 \cdot 6H_2O$), sodium carbonate (Na_2CO_3), ethanol (C_2H_5OH), aluminum nitrate nonahydrate ($Al(NO_3)_3 \cdot 9H_2O$) (Sigma-Aldrich). Sodium hydroxide (NaOH) and sodium chloride (NaCl) (Merck), as well as hydrochloric acid (HCl, LabGuard®), were used as received. Locally produced distilled water was used in all stages of synthesis and washing. The antibiotic ceftriaxone (CEF) was obtained from Bernofarm, Indonesia.

The material was characterized using various instruments, including an X-ray diffractometer (XRD, Rigaku MiniFlex 600) to evaluate its crystal structure, an FTIR spectrophotometer (Shimadzu Prestige-21) to identify functional groups, and a scanning electron microscope (SEM, Thermo Scientific Quattro) to observe the surface morphology. Specific surface area and pore distribution were determined using the Brunauer–Emmett–Teller (BET) method with a BET analyzer (Nova 2200e). Meanwhile, the concentration of ceftriaxone (CEF) was measured using a UV-Vis spectrophotometer (Biobase BK-UV 1800 PC series) at a wavelength of 240 nm.

2.2. Synthesis of Ni/Al LDH [38]

Ni/Al LDH was synthesized via the coprecipitation method. A 100 mL precursor solution containing 0.75 M $Ni(NO_3)_2.6H_2O$ and 0.25 M $Al(NO_3)_3.9H_2O$ was prepared in a beaker. Next, a mixture of 50 mL 2 M NaOH and 100 mL 2 M Na_2CO_3 was slowly added to the precursor solution while stirring, until the pH reached 10. The reaction suspension was then maintained at 80 °C with constant stirring for 17 hours. The formed precipitate is filtered, washed with distilled water, and then dried. The synthesized material was then analyzed using XRD, FTIR, SEM, and BET.

2.3. Green Tea (*Camellia sinensis*) Leaf Extraction

The extraction procedure for green tea leaves (*Camellia sinensis*) was carried out based on a modified method from Han *et al.* [39]. Fresh tea leaves are dried and ground into a fine powder. The extraction process was carried out using the maceration method with 96% ethanol as the solvent. The dried leaf powder was soaked in ethanol and left at room temperature for 1 hour. The resulting mixture was then filtered, and the ethanol solvent was removed using a rotary evaporator at 48 °C. The concentrated extract obtained was stored at low temperature until used for the material synthesis stage.

2.4. Preparation of Ni/Al-CS Composites

Ni/Al-CSe composite was synthesized using the coprecipitation method with natural material modification (referring to Luo *et al.* [40] with some adjustments). A precursor solution containing Ni^{2+} and Al^{3+} in a molar ratio of 5:1 was prepared in 200 mL of distilled water, then 0.5 g of CS leaf extract was added. Subsequently, 0.5 M NaOH solution was added dropwise until the pH reached 10, and the suspension was continuously stirred

for 24 hours until homogeneous. The formed precipitate is separated by filtration, washed with distilled water until neutral, and then dried in an oven. The resulting dry powder was used as a Ni/Al-CSe composite.

2.5. Determination of the point of zero charge (pH_{pzc})

The zero point of charge (pHpzc) of Ni/Al LDH and Ni/Al-CSe was determined using the pH drift method. A 20 mL solution of 0.1 M NaCl with an initial pH adjusted within the range of 2–10 (using 0.1 M HCl or 0.1 M NaOH) was mixed with 0.02 g of the sample. The mixture was stirred in a shaker for 24 hours at room temperature, and then the final pH was measured with a pH meter. The difference between the initial and final pH (ΔpH) is calculated, and the pHpzc value is obtained from the graph of the relationship between the initial pH and ΔpH at the intersection with the line ΔpH = 0.

2.6. Adsorption of CEF

Adsorption experiments were conducted to study the influence of several operating parameters, namely solution pH (3-10), contact time (10-120 minutes) for adsorption kinetics studies, initial CEF concentration (15-30 $mg.L^{-1}$) and temperature (30–50 °C) for isotherm and thermodynamic studies, as well as variations in adsorbent dosage (0.01-0.10 g). In each experiment, 20 mL of CEF solution was mixed with Ni/Al LDH or Ni/Al-CSe adsorbent, then shaken using a shaker until the predetermined contact time was reached. After the process is complete, the suspension is separated and the concentration of residual CEF is analyzed using a UV-Vis spectrophotometer at a wavelength of 240 nm. Regeneration studies were conducted for up to four cycles, observing the percentage adsorption results from the first to the last cycle. Additionally, desorption tests were conducted separately to understand the adsorption mechanism. At this stage, the adsorbed CEF was eluted using several reagents, namely distilled water (DW), NaOH, HCl, distilled water with ultrasonic assistance (DW+US), and ethanol (EtOH). The adsorption capacity (q_t) at time t is calculated using the following equation:

$$q_t = \frac{(C_0 - C_t)V}{m} \quad (1)$$

where, C_0 is initial concentration ($mg.L^{-1}$), C_t is concentration at time t ($mg.L^{-1}$), V is volume of CEF solution (L), and m is mass of adsorbent (g).

3. Results and Discussion

3.1. Characterization of the Adsorbent Materials

The XRD diffraction patterns for Ni/Al LDH and Ni/Al-CSe are shown in Figure 1(a). The Ni/Al LDH material exhibits characteristic peaks

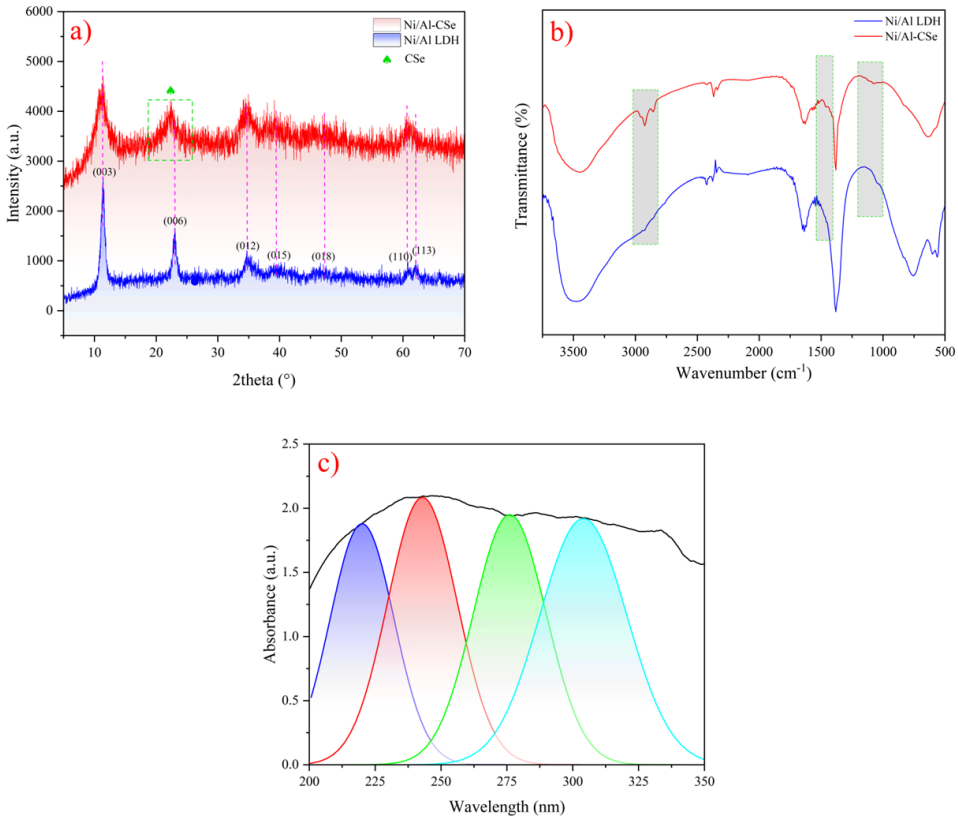

Figure 1. (a) XRD patterns and (b) FTIR spectra of Ni/Al LDH and Ni/Al–CSe, and (c) UV-Vis wavelength scan spectrum of CSe.

at 2θ angles of 11.39, 23, 34.86, 39.41, 47.30, 60.81, and 62.05 with crystal planes (003), (006), (012), (015), (018), (110), and (113), which are consistent with JCPDS reference data No. 15-0087, confirming the formation of the typical layered double hydroxide lamellar structure [41]. After modification with *Camellia sinensis* extract (Ni/Al-CSe), the XRD pattern still shows the main peaks of Ni/Al LDH, although the relative intensity has changed and a broader background has appeared around 2θ of 20–30°. This phenomenon indicates the contribution of amorphous organic compounds from the green tea leaf extract, which are dispersed on the surface or interact with the LDH layers [42].

The FT-IR spectra of Ni/Al LDH and Ni/Al-CSe can be seen in Figure 1(b). In Ni/Al LDH, the broad absorption band around 3450 cm^{-1} is related to the -OH stretching vibrations of hydroxyl groups within the LDH layers as well as water molecules trapped between them [43,44]. Meanwhile, the band at 1630 cm^{-1} originates from the bending vibration of H_2O molecules, and the intense band around 1380 cm^{-1} confirms the presence of nitrate anions (NO_3^-) which commonly occupy the interlayer space of LDH [45-47]. After modification with *Camellia sinensis* extract (Ni/Al-CSe), the spectrum shows additional bands in the region of 2920–2850 cm^{-1} related to C–H stretching from organic compounds, as well as bands around 1050–1100 cm^{-1} associated with C–O vibrations from phenolic or alcohol groups. The presence of this band indicates that the bioactive compounds from the green tea leaf extract were successfully immobilized on the material. The band appearing around 1465 cm^{-1} is related to the stretching of aromatic C=C, while the strong band at 1635 cm^{-1} can be attributed to the C=O vibration of flavonoids, polyphenols, and catechins. The broad band at 3284–3450 cm^{-1} reflects the O–H stretching of phenols and flavonoids [48]. Additionally, the absorption bands in the low wavenumber region <1000 cm^{-1} are associated with metal-oxygen vibrations (M-O, where M = Ni and Al) [28]. These bands persist in Ni/Al-CSe, confirming that the basic LDH structure remains intact after modification.

The CSe spectrum wavelength scan (Figure 1(c)) shows a broad absorption band in the range of 200-350 nm with four main deconvoluted peaks at 220, 243, 276, and 304 nm, indicating successful synthesis and the formation of active compounds in CSe. The peaks at 220 nm and 276 nm indicate the presence of catechin compounds, the dominant component in green tea extract, which are associated with $\pi \rightarrow \pi^*$ transitions in the benzene ring aromatic system [49]. The peak at 243 nm, which occurs within the range of 240-285 nm, can be attributed to electron transitions in the benzoyl band, while the peak at 304 nm, which occurs within the range of 300–385 nm, represents transitions in the cinnamoyl band in the flavonoid structure [50]. This absorption pattern confirms that the CSe contains catechin and flavonoid compounds with a strong conjugated aromatic system, which is an indicator of the successful synthesis process and the formation of bioactive components that have the potential to improve the performance of the Ni/Al-CSe material.

Morphological analysis using SEM (Figure 2a–b) reveals that Ni/Al LDH exhibits a platelet-like layered aggregate morphology with an average particle diameter of approximately 4.88 μm, as obtained from particle size distribution analysis. The particles form relatively compact aggregates, which are attributed to the restacking of LDH nanosheets during drying and sample preparation, leading to overlapping plate domains. After modification with *Camellia sinensis* extract (Ni/Al-CSe), the morphology becomes more heterogeneous with looser and less compact agglomeration, accompanied by an increase in the average particle size to 5.83 μm. This change is associated with the adsorption of organic components from the CSe on the LDH surface, which can act as a spacer between adjacent layers, modifying interparticle interactions and influencing the aggregation behavior. Consequently, particles with more irregular shapes and larger apparent sizes are formed compared to pristine LDH.

Characterization of pore texture thru nitrogen adsorption-desorption analysis (Figure 2(c)) shows that both materials have type IV isotherms with H3 hysteresis, which is characteristic of mesoporous materials (2-50 nm) [51,52]. However, pore texture parameters showed significant differences. Pure Ni/Al LDH has a high specific surface area of 83.89 m^2/g, with a pore volume of 0.23 cm^3/g and a pore size of 6.60 nm. After modification with CSe, the specific surface area value drastically decreased to 18.97 m^2/g, with a pore volume of 0.014 cm^3/g and a pore size of 3.40 nm.

This decrease in surface area can be explained by the presence of organic molecules from the CSe that partially cover the active sites or enter the LDH pore cavities, thus reducing nitrogen accessibility during BET analysis. However, the presence of these organic compounds can actually enrich the functional properties of the material thru the contribution of active groups such as –OH, –C=O, and aromatic bonds from polyphenols, making Ni/Al-CSe remain competitive and potentially superior in antibiotic adsorption applications compared to Ni/Al LDH.

3.2. Adsorption Study

Determining the point of zero charge (pH_{pzc}) is an important parameter for understanding the

surface charge properties of the adsorbent and understanding the mechanism of interaction with the adsorbate [53]. The pH_{pzc} values of Ni/Al LDH and Ni/Al-CSe, determined using the ΔpH method, are shown in Figure 3(a). The pH_{pzc} value for Ni/Al LDH was recorded at pH of 7.34, while Ni/Al-CSe showed a shift to a lower value, at pH 6.75. Figure 3(b) shows that the maximum adsorption capacity was achieved at pH of 3 for Ni/Al LDH and pH of 5 for Ni/Al-CSe. Under conditions where pH < pH_{pzc}, the adsorbent surface is positively charged, allowing for more effective electrostatic interactions with the negatively charged groups of ceftriaxone molecules (such as electron-rich aromatic rings) [54-56]. Conversely, at pH > pH_{pzc}, the adsorbent surface is negatively charged, leading to electrostatic repulsion with CEF molecules, which also tend to be negatively charged under basic conditions.

Additionally, Ni/Al-CSe exhibited higher adsorption capacity compared to Ni/Al LDH across the entire pH range. This can be attributed to the contribution of bioactive compounds from the tea leaf extract, which contains polyphenols and flavonoids, acting as additional sites for

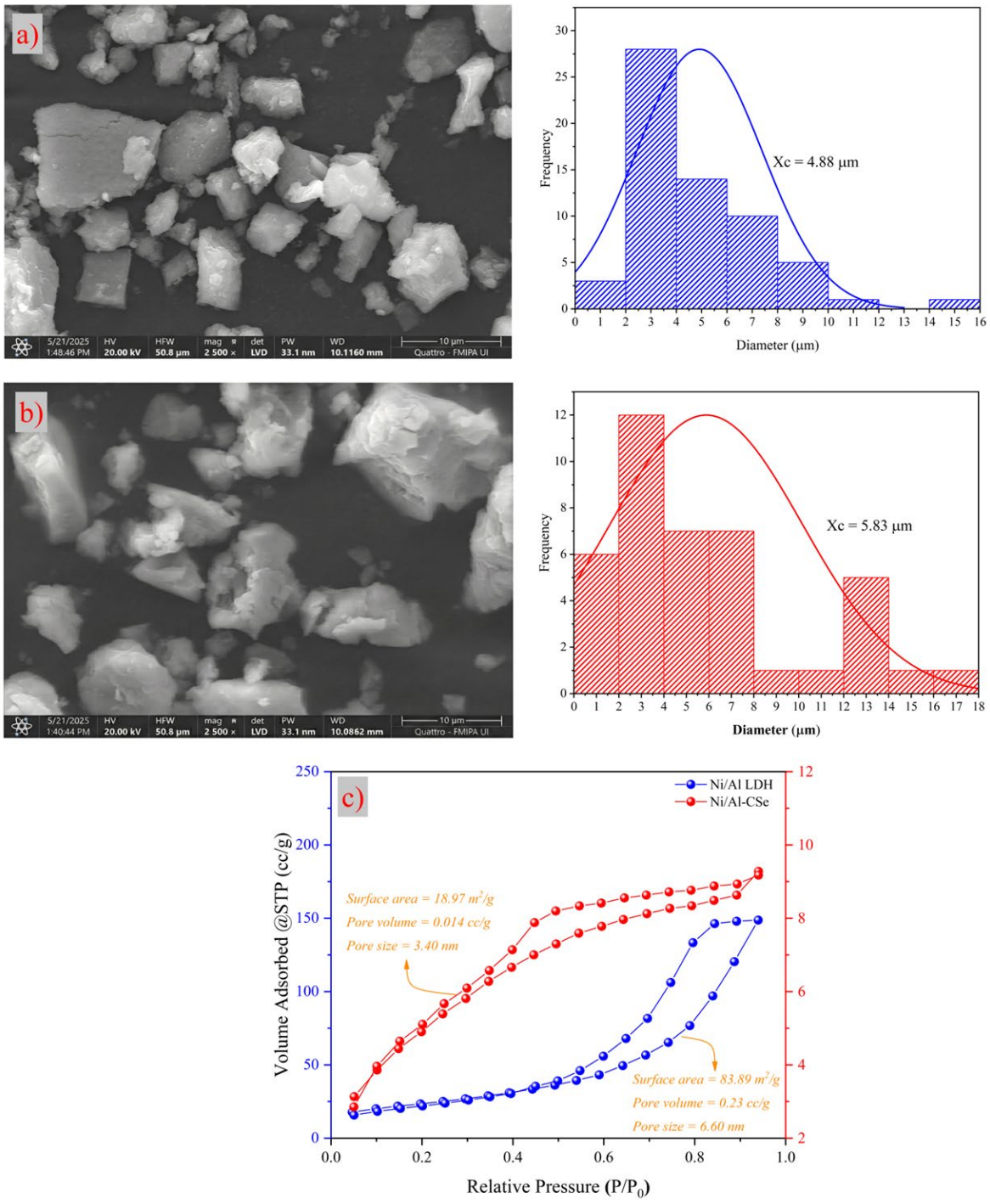

Figure 2. SEM images and particle size distributions of (a) Ni/Al LDH and (b) Ni/Al-CSe, and (c) N_2 adsorption–desorption isotherms (BET analysis) of both materials.

interaction with antibiotics. Thus, modification of LDH Ni/Al using CSe not only affects surface properties (pH_{pzc}) but also enhances overall adsorption capacity.

The adsorption behavior of CEF by Ni/Al LDH and Ni/Al-CSe as a function of time can be seen in Figure 4(a). Both materials show a fairly sharp increase in adsorption capacity in the initial stage (0-40 minutes) due to the abundance of active sites still available on the surface. As time goes on, the rate of adsorption decreases and reaches equilibrium at around the 75th minute. After that point, the adsorption capacity remains relatively constant, indicating that most of the active sites have been occupied, resulting in no significant additional adsorption. At equilibrium, the maximum adsorption capacity recorded was 13.25 mg/g for Ni/Al LDH and 14.50 mg/g for Ni/Al-CSe. The higher adsorption performance of Ni/Al-CSe compared to Ni/Al LDH can be explained by the presence of CS leaf extract (CSe), which is rich in active groups, enabling it to act as an additional binding site that strengthens the interaction between the material surface and CEF molecules.

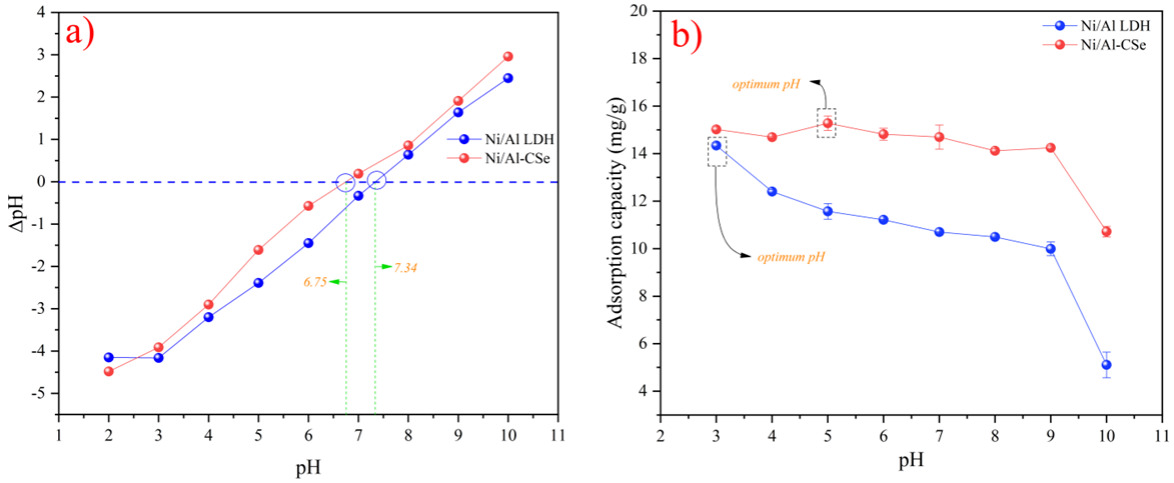

Figure 3. (a) Determination of point of zero charge (pH_{pzc}) of Ni/Al LDH and Ni/Al-CSe. (b) Effect of solution pH on the adsorption capacity of ceftriaxone using Ni/Al LDH and Ni/Al-CSe.

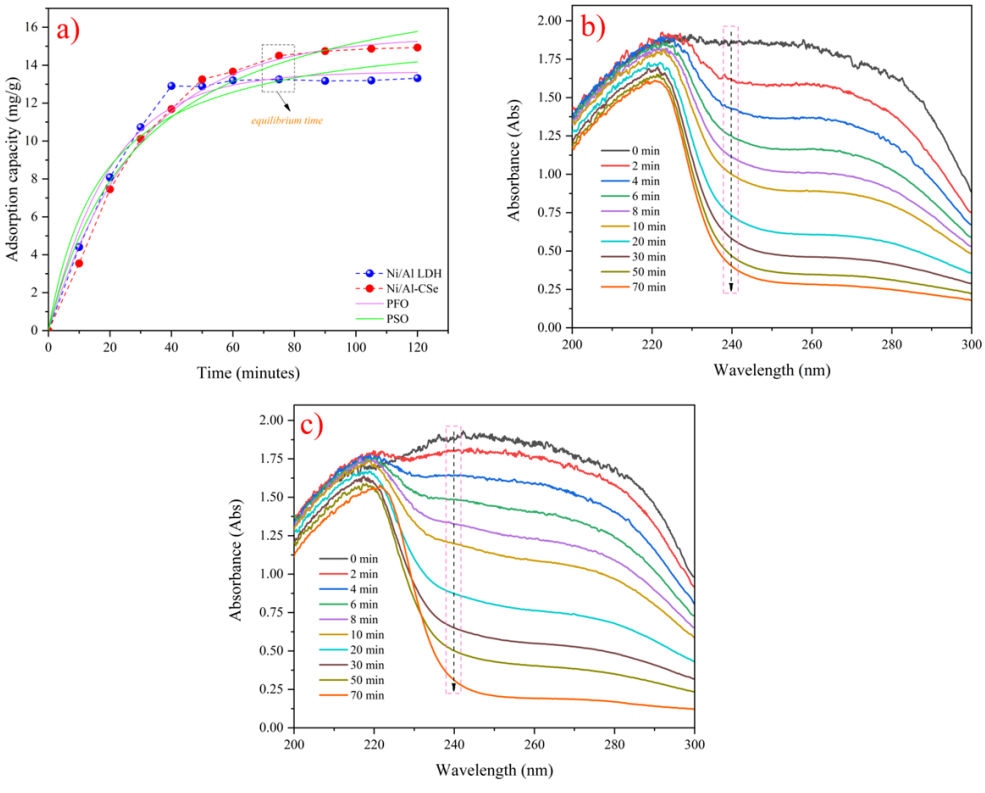

Figure 4. (a) The effect of time and adsorption kinetic modeling using PFO and PSO models for Ni/Al LDH and Ni/Al-CSe. UV–Vis spectral changes of ceftriaxone during adsorption using (b) Ni/Al LDH and (c) Ni/Al-CSe at different contact times (0–70 min).

To understand the adsorption kinetics mechanism, the experimental data were analyzed using the pseudo-first-order (PFO) and pseudo-second-order (PSO) models, as shown in Table 1. The PFO model yielded higher values of the coefficient of determination (R^2), namely 0.985 (Ni/Al LDH) and 0.994 (Ni/Al-CSe), compared to the PSO, which were 0.961 and 0.982, respectively. Additionally, the calculated equilibrium adsorption capacity value (q_e(calc)) for PFO is also more consistent with the experimental value (q_e(exp)), which is 13.652±0.296 mg.g^{-1} (LDH) and 15.517±0.281 mg.g^{-1} (CSe), approaching the actual values of 13.317 mg/g and 14.932 mg.g^{-1}. Based on the data, it can be concluded that the PFO model is more suitable for describing the adsorption kinetics of CEF on both materials. This indicates that the adsorption process is controlled by a physical mechanism (physisorption) that is dominant in the initial stages, although the presence of active groups from the CS leaf extract on Ni/Al-CSe also contributes thru chemical interactions that strengthen the bond with ceftriaxone molecules.

Figure 4(b-c) shows the changes in the UV-Vis spectrum of ceftriaxone (CEF) in the wavelength range of 200–300 nm during the adsorption process using Ni/Al LDH (Figure 4(b)) and Ni/Al-CSe (Figure 4(c)). Initially (0 minutes), the CEF solution showed high absorbance intensity with a main peak around 240 nm. As the contact time increased, the absorbance intensity gradually decreased for both materials, indicating a reduction in CEF concentration due to the adsorption process. In the Ni/Al LDH system (Figure 4(b)), the absorbance decreased progressively until the 70th minute, resulting in a removal percentage of 79.61%. Meanwhile, Ni/Al-CSe (Figure 4(c)) showed a more significant decrease in absorbance compared to Ni/Al LDH. At the 70th minute, the removal efficiency reached 83.52%. This increase can be attributed to the presence of bioactive compounds in green tea leaf extract (*Camellia sinensis*), such as polyphenols and flavonoids, which enrich the surface functional groups. The presence of these functional groups strengthens hydrogen bonds and increases the adsorbent's affinity for ceftriaxone molecules, while also increasing the effective surface area due to better particle distribution. These two results indicate that the adsorption process of ceftriaxone is rapid in the initial stage (0–20 minutes), which suggests the dominance of surface interactions and the abundance of available active sites. After that period, the rate of absorbance decrease slowed down, indicating that conditions close to equilibrium were reached due to a reduction in available active sites.

Figure 5(a) shows the effect of adsorbent dosage variation on adsorption capacity (q_e), while Figure 5(b) illustrates the removal efficiency (%) of ceftriaxone using Ni/Al LDH and Ni/Al-CSe materials. In Figure 5(a), the adsorption capacity (q_e) tends to decrease with increasing adsorbent dosage. At a dosage of 0.01 g, the q_e value reached 90.31 mg/g (Ni/Al LDH) and 95.34 mg.g^{-1} (Ni/Al-CSe). However, when the dosage increased to 0.1 g, the adsorption capacity decreased to 10.42 mg.g^{-1} (Ni/Al LDH) and 14.44 mg.g^{-1} (Ni/Al-CSe). This decrease is caused by an excess of active sites at high dosages, while the number of CEF molecules in the solution is limited. Additionally, particle agglomeration at high adsorbent concentrations can reduce the effective surface area, thereby decreasing the adsorption capacity per gram [57].

Figure 5(b) shows different trends for both materials. For Ni/Al LDH, the removal efficiency increased up to an optimum dosage of 0.04 g with a value of 79.36%, then decreased at higher dosages, reaching 64.83% at 0.1 g. This decrease can be explained by particle agglomeration and overlapping active sites, which reduce adsorption effectiveness. Conversely, Ni/Al-CSe showed a more stable increasing trend in efficiency, from 59.28% (0.01 g) to 89.86% (0.1 g). This indicates that Ni/Al-CSe, with an increased adsorbent dosage, provides a greater total number of active sites, allowing more adsorbate molecules in the

Table 1. Kinetics parameters of CEF adsorption on Ni/Al LDH and Ni/Al-CSe.

Parameters	Ni/Al LDH	Ni/Al-CSe
Pseudo first order		
k_1 (min^{-1})	0.0494±0.042	0.0341±0.281
q_e (calc) (mg.g^{-1})	13.652±0.296	15.517±0.281
R^2	0.985	0.994
Pseudo second order		
k_2 (min.g.mg^{-1})	0.00351±0.00098	0.00168±0.00034
q_e (calc) (mg.g^{-1})	16.250±0.938	19.736±1.022
R^2	0.961	0.982
q_e (exp)	13.317	14.932

solution to bind, although the adsorption capacity per gram of adsorbent decreases. These results indicate that the Ni/Al-CSe material has better performance compared to Ni/Al LDH in terms of both adsorption capacity and removal efficiency percentage. Ni/Al-CSe consistently showed higher adsorption capacity and greater removal efficiency across all adsorbent dosage variations, confirming that modification with CS leaf extract can improve the material's performance in the ceftriaxone adsorption process.

Table 2 presents the Langmuir and Freundlich isotherm parameters for the adsorption process of CEF using Ni/Al LDH and Ni/Al-CSe at a temperature of 303 K. The analysis results show that the maximum adsorption capacity (q_{max}) obtained from the Langmuir model significantly increased after the material was modified with green tea leaf extract. The q_{max} value for Ni/Al LDH was recorded as 28.818 mg.g^{-1}, while Ni/Al-CSe reached 111.111 mg.g^{-1}, which is approximately four times higher. This increased capacity indicates that the presence of bioactive compounds from CS extract, such as polyphenols and flavonoids, plays a role in enriching the surface active sites and enhancing the specific interaction between the adsorbent and antibiotic molecules. Although both isotherm models were evaluated, the Langmuir model was applied to determine the maximum adsorption capacity (q_{max}), since this parameter is exclusively defined within the Langmuir framework and cannot be obtained from the Freundlich model.

The correlation coefficient (R^2) indicates that the adsorption data for Ni/Al LDH is more consistent with the Freundlich model (R^2 = 0.757) compared to the Langmuir model (R^2 = 0.712). Similarly, for Ni/Al-CSe, the Freundlich model also provides a better fit (R^2 = 0.891) compared to the Langmuir model (R^2 = 0.180). Thus, the mechanism of ceftriaxone adsorption on the modified material more dominantly follows a multilayer adsorption pattern on a heterogeneous surface [58,59]. Additionally, the value of n obtained for Ni/Al-CSe (1.167) is closer to 1 compared to Ni/Al LDH (1.946). The value of n < 2 for both materials indicates that the adsorption process occurs with moderate to relatively weak interaction strength, but still proceeds spontaneously [60]. Additionally, the 1/n values for both materials are less than 1 (0 < 1/n < 1), indicating that the CEF removal process is more

Table 2. Adsorption isotherm parameters of CEF using Ni/Al LDH and Ni/Al-CSe.

Materials	T(°K)	Parameters			
		Isoterm Langmuir		Isoterm Freundlich	
Ni/Al LDH	303	q_{max} (mg.g^{-1})	28.818	n	1.946
				1/n	0.514
		K_L (L.mg^{-1})	0.106	K_F [(mg.g^{-1})(L.mg^{-1})$^{1/n}$]	4.509
		R^2	0.712	R^2	0.757
Ni/Al-CSe	303	q_{max} (mg.g^{-1})	111.111	n	1.167
				1/n	0.857
		K_L (L.mg^{-1})	0.025	K_F [(mg.g^{-1})(L.mg^{-1})$^{1/n}$]	3.148
		R^2	0.180	R^2	0.891

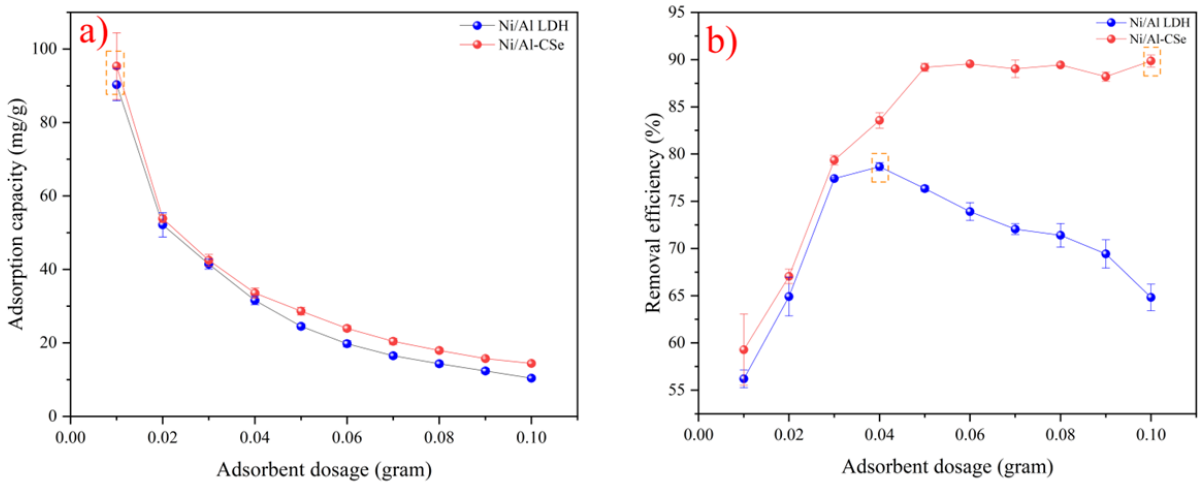

Figure 5. Effect of adsorbent dosage on (a) adsorption capacity (q_e) and (b) removal efficiency (%) of ceftriaxone using Ni/Al LDH and Ni/Al-CSe.

favorable. If the 1/n value is 1, it indicates no interaction between the adsorbate and adsorbent throughout the adsorption mechanism; and if 1/n > 1, it indicates that the adsorption process is difficult to occur [61]. To evaluate the performance of the synthesized material, a comparison with other previously reported adsorbents is shown in Table 3.

The thermodynamic parameters presented in Table 4 provide further insight into the mechanism of CEF adsorption on Ni/Al LDH and Ni/Al-CSe. The variation of Gibbs free energy change (ΔG) with temperature provides insight into the effect of thermal energy on adsorption spontaneity. As shown in Table 4, all ΔG values remain negative over the temperature range of 303–323 K, confirming that CEF adsorption on both Ni/Al LDH and Ni/Al-CSe proceeds spontaneously at all studied concentrations (15–30 mg/L) [28]. For Ni/Al LDH, ΔG becomes more negative with increasing temperature at 15 and 30 mg/L, indicating enhanced spontaneity at higher temperatures, whereas at 20 and 25 mg/L the ΔG values gradually become less negative, suggesting a slight decrease in adsorption favorability upon heating. A similar trend is observed for Ni/Al-CSe, where the ΔG values decrease with increasing temperature at 15 and 30 mg/L, but show a slight increase (less negative values) at 20 and 25 mg/L. Nevertheless, across all temperatures and concentrations, Ni/Al-CSe consistently exhibits more negative ΔG values than Ni/Al LDH, demonstrating superior thermodynamic favorability and stronger affinity toward CEF.

The enthalpy changes (ΔH) reveal differences in adsorption mechanisms for both adsorbents depending on concentration. For Ni/Al LDH, positive ΔH values are observed at 15 and 30 mg/L (0.813 and 2.517 kJ/mol), suggesting endothermic adsorption behavior, whereas negative ΔH values at 20 and 25 mg/L (-7.685 and -2.080 kJ/mol) indicate an exothermic contribution under these conditions. In contrast, Ni/Al-CSe displays predominantly negative ΔH values throughout the experimental concentration range (-1.666 to -9.490 kJ/mol), reflecting mainly exothermic adsorption processes. This behavior implies that the incorporation of bioactive compounds from green tea leaf extract contributes to the formation of energetically favorable adsorption sites, thereby facilitating CEF immobilization on the modified surface.

Table 3. Comparison of maximum adsorption capacities (Q_m) of Ni/Al LDH and Ni/Al-CSe for ceftriaxone with other adsorbents reported in the literature.

Adsorbent	Target adsorbate	Isotherm model	Q_m (mg.g^{-1})	Reference
Chitosan-GO-Zr	Ceftriaxone	Langmuir	32.25	[12]
Fe_3O_4-lignin	Ceftriaxone	Langmuir	86	[54]
Fe_3O_4-carbon-based lignin	Ceftriaxone	Freundlich	87	[54]
Powder activated carbon modified with magnetite nanoparticles (PAC-MNPs)	Ceftriaxone	Langmuir	28.93	[55]
C_3N_4/MWCNT/Bi_2WO_6	Ceftriaxone	Langmuir	19.57	[62]
Spent coffee grounds	Ceftriaxone	Langmuir	14.2	[60]
NBent-NTiO_2-Chit	Ceftriaxone	Langmuir	90.91	[4]
GO derived corn cob	Ceftriaxone	Freundlich	3.02	[63]
Pseudomonas putida biomass	Ceftriaxone	Freundlich	109.5	[64]
CuO nanosphere	Ceftriaxone	Langmuir	127	[61]
Ni/Al LDH	Ceftriaxone	Freundlich	28.818	This study
Ni/Al-CSe	Ceftriaxone	Freundlich	111.11	This study

Table 4. Thermodynamic parameter values for CEF adsorption on Ni/Al LDH and Ni/Al-CSe.

Materials	Concentration (mg/L)	ΔH (kJ/mol)	ΔS (kJ/mol.K)	ΔG (kJ/mol)		
				303	313	323
Ni/Al LDH	15	-0.813	0.002	-1.387	-1.406	-1.425
Ni/Al-CSe		5.862	0.026	-2.153	-2.417	-2.682
Ni/Al LDH	20	-7.685	-0.020	-1.643	-1.444	-1.244
Ni/Al-CSe		-9.490	-0.023	-2.550	-2.321	-2.092
Ni/Al LDH	25	-2.080	-0.005	-0.716	-0.671	-0.626
Ni/Al-CSe		-3.502	-0.005	-1.965	-1.914	-1.863
Ni/Al LDH	30	2.517	0.011	-0.866	-0.978	-1.089
Ni/Al-CSe		-1.666	0.002	-2.222	-2.240	-2.259

Entropy changes (ΔS) further clarify the physicochemical nature of adsorption. For Ni/Al LDH, the ΔS values range from −0.020 to 0.011 kJ/mol.K over the investigated concentration range (15–30 mg/L), indicating that the adsorption process may involve either slight increases or decreases in interfacial disorder depending on CEF concentration. Similarly, Ni/Al-CSe exhibits both positive and negative ΔS values (-0.023 to 0.026 kJ/mol.K), reflecting concentration-dependent variations in randomness at the solid–solution interface. Positive ΔS values suggest increased degrees of freedom of adsorbed species, whereas negative ΔS values imply the formation of a more ordered adsorption system due to stronger and more specific interactions between CEF molecules and the surface functional groups introduced by the green tea extract modification [65]. These thermodynamic features are consistent with the more negative ΔG values obtained for Ni/Al-CSe, confirming its superior adsorption affinity toward CEF.

The adsorbent's regeneration ability is one of the important parameters for assessing its application potential in sustainable waste treatment. Figure 6(a) shows the results of the regeneration test of Ni/Al LDH and Ni/Al-CSe materials for CEF adsorption up to four reuse cycles. In the first cycle, both materials showed relatively high adsorption efficiency, namely 75.8% for Ni/Al LDH and 77.03% for Ni/Al-CSe. This indicates that modification with green tea leaf extract provides competitive initial performance compared to unmodified materials. As the number of cycles increases, there is a decrease in adsorption efficiency for both materials. However, Ni/Al-CSe consistently showed better performance compared to Ni/Al LDH. In the second cycle, the efficiency of Ni/Al-CSe remained at 69.98%, which was higher than Ni/Al LDH at 63.86%. Similar trends were observed in the third and fourth cycles, where Ni/Al-CSe recorded efficiencies of 64.18% and 58.12%, respectively, while Ni/Al LDH only achieved 52.75% and 46.74%. This difference in regeneration performance can be attributed to the presence of bioactive compounds from CS extract integrated into the LDH structure. These compounds are believed to enhance surface stability and prevent the loss of most active sites during repeated adsorption processes.

3.3. Mechanism of Adsorption

Figure 6(b) shows the results of ceftriaxone (CEF) desorption tests from Ni/Al LDH and Ni/Al-CSe materials using various reagents, namely distilled water (DW), NaOH, HCl, distilled water with ultrasound (DW+US), and ethanol (EtOH). This test is conducted to help explain the adsorption mechanism occurring between CEF and the material. The results show that NaOH and HCl reagents provide the highest desorption values. When using NaOH, the desorption percentage reaches 88.31% for Ni/Al LDH and 88.51% for Ni/Al-CSe. This indicates that electrostatic interactions play an important role in the adsorption process. When using HCl, the desorption values are even higher, namely 93.20% (Ni/Al LDH) and 95.71% (Ni/Al-CSe). However, observations indicate that the material undergoes structural damage under strong acidic conditions. Thus, the high desorption in HCl not only reflects the release of CEF due to disruption of electrostatic interactions, but also due to the degradation of the LDH layer, which is inherently unstable in acidic conditions. Therefore, desorption data with NaOH is more

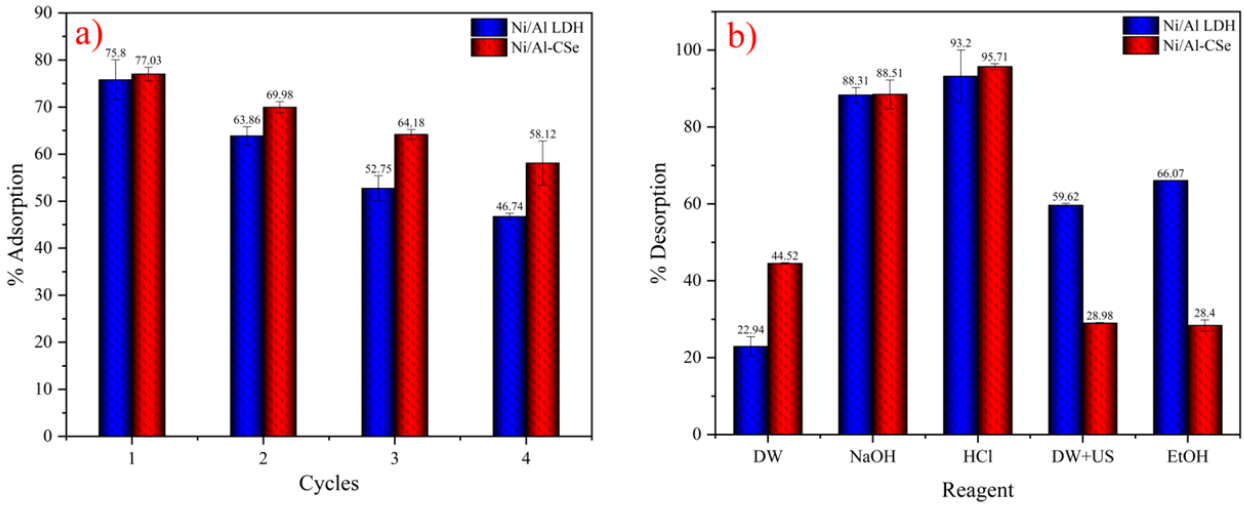

Figure 6. (a) Regeneration performance of Ni/Al LDH and Ni/Al-CSe for ceftriaxone adsorption and (b) Desorption efficiency of ceftriaxone from Ni/Al LDH and Ni/Al-CSe using different reagents.

representative in explaining the interaction mechanism between CEF and the adsorbent.

Other reagents showed lower desorption values. The use of DW and EtOH resulted in limited release, only 22.94% and 66.07% respectively for Ni/Al LDH, and 44.52% and 28.40% for Ni/Al-CSe. This indicates that neither hydrophobic interactions nor hydrogen bonds are the dominant mechanism in CEF adsorption. Meanwhile, the use of DW with ultrasound (DW+US) resulted in moderate desorption, namely 59.62% (Ni/Al LDH) and 28.98% (Ni/Al-CSe). Ultrasonic vibrations help release some of the weakly bound molecules on the surface, but they are not strong enough to break electrostatic bonds. These desorption results confirm that the main mechanism of CEF adsorption on both Ni/Al LDH and Ni/Al-CSe is primarily controlled by electrostatic interactions, with additional contributions from other surface interactions. The fact that Ni/Al-CSe still exhibits high desorption values in NaOH without structural damage confirms that modification with CS extract not only enhances adsorption performance but also maintains material stability.

The FT-IR spectrum after CEF adsorption shown in Figure 7(a) exhibits several significant changes. The intensity of the -OH band at 3400 cm^{-1} decreases, indicating the involvement of hydroxyl groups in hydrogen interactions with CEF. The shift and increase in intensity of the band around 1630-1700 cm^{-1} suggest the contribution of carbonyl (C=O) groups from CEF interacting with the adsorbent surface. Additionally, the band around 1200-1300 cm^{-1} associated with C–O–C stretching undergoes intensity changes, confirming the presence of bonds between the ether/ester groups of CEF and the active sites of the adsorbent. The metal-oxygen (M-O) bands located at <1000 cm^{-1} also experienced a slight shift after adsorption, indicating the possible occurrence of electrostatic interactions between the CEF anions and the cationic LDH layer. Overall, these findings support the conclusion that the mechanism of CEF adsorption on Ni/Al-CSe occurs thru a combination of hydrogen bonding, electrostatic interactions, and the contribution of aromatic organic interactions (π-π stacking) mediated by bioactive compounds from CS extract. The possible mechanism of CEF adsorption that occurs can be seen in Figure 7(b).

4. Conclusions

This research confirms that the bio-modification of Ni/Al LDH with *Camellia sinensis* extract significantly enhances the adsorption performance of ceftriaxone. The pH optimum shifted from 3 for Ni/Al LDH to 5 for Ni/Al-CSe, with the isotherm following the Freundlich model and the kinetics conforming to pseudo-first order. The maximum adsorption capacity increased from 28.818 $mg.g^{-1}$ to 111.111 $mg.g^{-1}$, indicating the significant role of bioactive groups in strengthening the interaction with CEF. Thermodynamic analysis revealed that adsorption on both materials proceeds spontaneously, while the more negative ΔG values and predominantly exothermic behavior of Ni/Al-CSe confirm its superior thermodynamic favorability associated with more specific surface interactions. Regeneration tests prove that Ni/Al-CSe is more stable than Ni/Al LDH for up to four cycles. Overall, these results confirm that bio-modification with *Camellia sinensis* extract is an effective and sustainable strategy for addressing antibiotic pollution in aquatic environments.

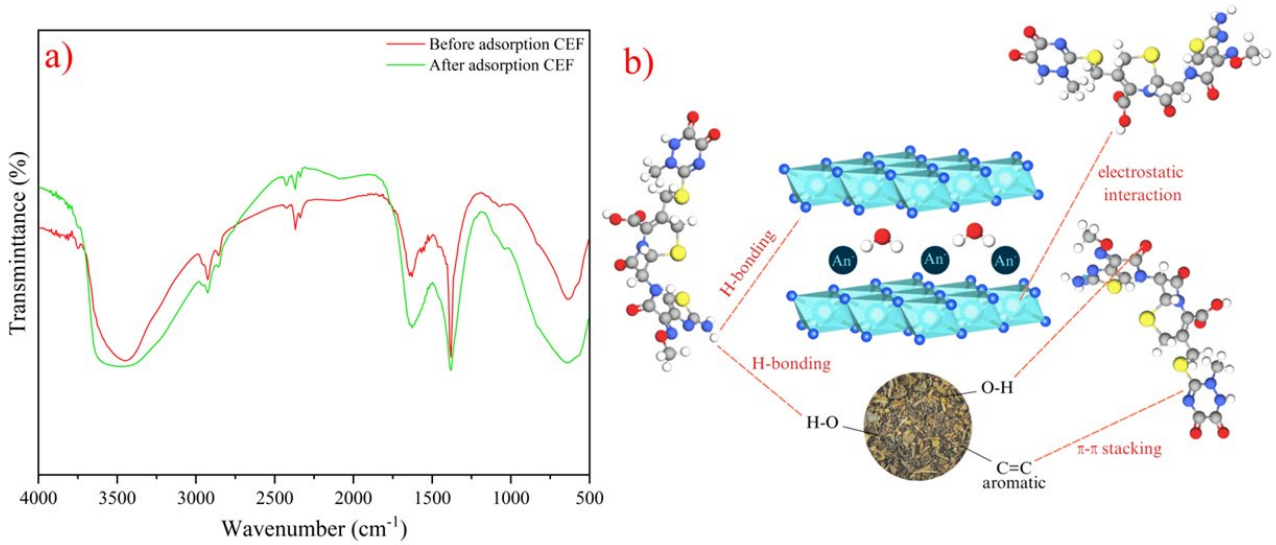

Figure 7. (a) FTIR spectra of Ni/Al-CSe before and after CEF adsorption and (b) Schematic diagram of the possible mechanism of CEF adsorption on Ni/Al-CSe.

Acknowledgment

The authors would like to thank the Research Center of Inorganic Materials and Coordination Complexes, Universitas Sriwijaya, for their support and facilities.

CRedit Author Statement

Author Contributions: Amri Amri: Investigation, Writing – Original draft, Writing – review & editing, Software, Formal Analysis; Najma Annuria Fithri: Data Curation, Formal Analysis, Validation; Muhammad Said: Formal Analysis, Validation, Visualization, Data Curation; Aldes Lesbani: Methodology, Conceptualization, Writing – review & editing, Supervision, Validation, Visualization, Data Curation. All authors have read and agreed to the published version of the manuscript.

References

[1] Almuntashiri, A., Jiang, J., Hosseinzadeh, A., Badeti, U., Navidpour, A.H., Dorji, P., Ghaffour, N., Shon, H.K., Phuntsho, S. (2025). Removal of antibiotics from a biologically nitrified human urine using granular activated carbon adsorption for a safe nutrient recovery in a circular economy. *Process Safety and Environmental Protection*, 201, 107516. DOI: 10.1016/j.psep.2025.107516.

[2] Xu, X., Dong, H., Liu, J., Zhuang, J., Huang, T., Gan, Y., Wu, B. (2025). Phosphate-ligand engineered biochar with electron-donor and nanoconfinement effects for selective antibiotic adsorption. *Chemical Engineering Journal*, 522, 167713. DOI: 10.1016/j.cej.2025.167713.

[3] He, W., Wan, S., Xu, M., Wei, W., Wang, D., Yi, C., Zhao, Y. (2025). A comprehensive study on the impact of UV aging time on the adsorption and desorption behaviors of antibiotics on degradable and non-degradable microplastics. *Journal of Environmental Chemical Engineering*, 13(5), 118271. DOI: 10.1016/j.jece.2025.118271.

[4] Mahmoud, M.E., El-Ghanam, A.M., Mohamed, R.H.A., Saad, S.R. (2020). Enhanced adsorption of Levofloxacin and Ceftriaxone antibiotics from water by assembled composite of nanotitanium oxide/chitosan/nano-bentonite. *Materials Science and Engineering: C*, 108, 110199. DOI: 10.1016/j.msec.2019.110199.

[5] Zhang, H., Xiao, Y., Peng, Y., Tian, L., Wang, Y., Tang, Y., Cao, Y., Wei, Z., Wu, Z., Zhu, Y., Guo, Q. (2023). Selective degradation of ceftriaxone sodium by surface molecularly imprinted BiOCl/Bi3NbO7 heterojunction photocatalyst. *Separation and Purification Technology*, 315, 123716. DOI: 10.1016/j.seppur.2023.123716.

[6] Guan, H., Li, Q., Liu, J., Liu, W., Wan, J. (2025). Hollow-Co3O4-C dodecahedrons derived from ZIF-67 composited with skimmed cotton carbon as cathode for electrocatalytic degradation of ceftriaxone sodium. *Applied Surface Science*, 701, 163291. DOI: 10.1016/j.apsusc.2025.163291.

[7] Feng, X., Shi, H., Liu, W., Ma, F., Liu, P., Wan, J. (2024). Flower-like Ni/Mn/MC microspheres derived from metal-organic frameworks for electrocatalytic degradation of ceftriaxone sodium. *Chemosphere*, 352, 141405. DOI: 10.1016/j.chemosphere.2024.141405.

[8] Tang, Y., Zhang, X., Huang, Y. (2025). Highly active Bi2O3/Co3O4 heterostructure peroxidase-mimicking nanozyme for the sensitive detection of ceftriaxone sodium antibiotic. *Microchemical Journal*, 209, 112902. DOI: 10.1016/j.microc.2025.112902.

[9] Li, Z., Zhang, H., Deng, Q., Han, C., Zhang, C. (2025). Phosphate-adsorbed metal organic framework as a recycled material for catalytic degradation of ceftriaxone sodium via peroxymonosulfate activation. *Journal of Colloid and Interface Science*, 684, 390–402. DOI: 10.1016/j.jcis.2025.01.022.

[10] Chen, J.-L., Song, J.-F., Hao, H.-M., Zhou, S.-Y., Zhu, H.-Y., Zhang, X.-Q. (2025). Zinc-based polymers with N-heterocyclic ligands: multifunctional fluorescent sensors for Fe3+, Cr2O72- and ceftriaxone sodium (CRO). *Journal of Molecular Structure*, 1340, 142485. DOI: 10.1016/j.molstruc.2025.142485.

[11] Abbas, K.K., AbdulkadhimAl-Ghaban, A.M.H., Rdewi, E.H. (2022). Synthesis of a novel ZnO/TiO2-nanorod MXene heterostructured nanophotocatalyst for the removal pharmaceutical ceftriaxone sodium from aqueous solution under simulated sunlight. *Journal of Environmental Chemical Engineering*, 10(4), 108111. DOI: 10.1016/j.jece.2022.108111.

[12] Jafarzadeh, N., Jaafari, J., Moslemzadeh, M., Taghavi, K. (2025). A novel chitosan/graphene oxide nanocomposite functionalized with zirconium to remove dexamethasone and ceftriaxone from aqueous solutions: Response surface methodology, isotherm, kinetic and thermodynamic. *Journal of Water Process Engineering*, 69, 106722. DOI: 10.1016/j.jwpe.2024.106722.

[13] Hashemi, M., Rahimi, F., Abolghasemi, S., Nasiri, A., Rajabi, S. (2025). Revealing efficacy of AgCuFe2O4@GO/MnO2 in 3D electrochemical oxidation for ceftriaxone degradation in aqueous media: Optimization and mechanisms. *Environmental Technology & Innovation*, 37, 103914. DOI: 10.1016/j.eti.2024.103914.

[14] Yuliasari, N., Badri, A.F., Wijaya, A., Siregar, P.M.S.B.N., Amri, A., Mardiyanto, M., Mohadi, R., Lesbani, A. (2022). Modification of Mg/Al-LDH Intercalated Metal Oxide (Mg/Al-Ni) to Improve The Performance of Methyl Orange and Methyl Red Dyes Adsorption Process. *Science and Technology Indonesia*, 7(3), 275–283. DOI: 10.26554/sti.2022.7.3.275-283.

[15] Mohadi, R., Amri, A., Badaruddin, M., Ahmad, N., Lesbani, A. (2023). Adsorption of Phenol from Aqueous Solution Using Zn/Al Layered Double Hydroxides-Cellulose Composite. *Science and Technology Indonesia*, 8(1), 123–128. DOI: 10.26554/sti.2023.8.1.123-128.

[16] Nan, H., Luo, D., Zhang, X., Wang, J., Wang, C. (2025). Ca/La layered double hydroxide functionalized biochar: Preparation, characterization, phosphate adsorption mechanism, and post-evaluation of phosphorus availability. *Materials Today Communications*, 48, 113296. DOI: 10.1016/j.mtcomm.2025.113296.

[17] Yan, X., Deng, Y., Huang, W., Zhang, Q., Zheng, L., Zhou, J., He, D., Ma, J. (2025). Effect of preparation condition of Mg-Al layered double hydroxides on glyphosate adsorption and process optimization through response surface methodology. *Applied Clay Science*, 276, 107953. DOI: 10.1016/j.clay.2025.107953.

[18] Boucif, F., Bessaha, F., Bendahma, F., Bessaha, G., Mahrez, N., Sillanpää, M., Khelifa, A. (2025). Facile synthesis and modification of layered double hydroxides (LDH) for adsorption of Orange I and Acid Red 114 dyes from aqueous solution: Performance and mechanism study. *Inorganic Chemistry Communications*, 178, 114673. DOI: 10.1016/j.inoche.2025.114673.

[19] Lesbani, A., Ahmad, N., Mohadi, R., Royani, I., Wibiyan, S., Amri, Hanifah, Y. (2024). Selective adsorption of cationic dyes by layered double hydroxide with assist algae (Spirulina platensis) to enrich functional groups. *JCIS Open*, 15, 100118. DOI: 10.1016/j.jciso.2024.100118.

[20] Lesbani, A., Asri, F., Palapa, N.R., Taher, T., Rachmat, A. (2020). Efficient removal of methylene blue by adsorption using composite based ca/al layered double hydroxide-biochar. *Global Nest Journal*, 22(2), 250–257. DOI: 10.30955/gnj.003359.

[21] Palapa, N.R., Juleanti, N., Normah, Mohadi, R., Taher, T., Rachmat, A., Lesbani, A. (2020). Copper Aluminum Layered Double Hydroxide Modified by Biochar and its Application as an Adsorbent for Procion Red. *Journal of Water and Environment Technology*, 18(6), 359–371. DOI: 10.2965/jwet.20-059.

[22] Amri, A., Lesbani, A., Mohadi, R. (2023). Malachite Green Dye Adsorption from Aqueous Solution using a Ni/Al Layered Double Hydroxide-Graphene Oxide Composite Material. *Science and Technology Indonesia*, 8(2), 280–287. DOI: 10.26554/sti.2023.8.2.280-287.

[23] Asl, S.Z., Hooriabad Saboor, F., Seifzadeh, D., Safajou-Jahankhanemlou, M., Asgari, M. (2025). Layered double hydroxide-metal organic framework nanocomposites: A review on their versatile applications in electrocatalysts, supercapacitors, and adsorption. *Journal of Molecular Structure*, 1342, 142703. DOI: 10.1016/j.molstruc.2025.142703.

[24] Mubarak, M.F., Yousef, T.A., Salim, S.A., Khairy, M., Kamoun, E.A., Mahmoud, T. (2025). Meta-kaolinite metal oxide quaternary composite for layered double hydroxide applied to a new frontier in adsorption technology: Synthesis, adsorption performance and kinetics study. *Inorganic Chemistry Communications*, 178, 114647. DOI: 10.1016/j.inoche.2025.114647.

[25] Lesbani, A., Siregar, P.M.S.B.N., Palapa, N., Taher, T., Riyanti, F. (2021). Adsorptive Removal Methylene-Blue Using Zn/Al LDH Modified Rice Husk Biochar. *Polish Journal of Environmental Studies*, 30(4), 3117–3124. DOI: 10.15244/pjoes/130971.

[26] Wibiyan, S., Royani, I., Ahmad, N., Lesbani, A. (2024). Assessing the efficiency, selectivity, and reusability of ZnAl-layered double hydroxide and Eucheuma cottonii composite in removing anionic dyes from wastewater. *Inorganic Chemistry Communications*, 170, 113347. DOI: 10.1016/j.inoche.2024.113347.

[27] Wijaya, A., Ahmad, N., Hanum, L., Melwita, E., Hanifah, Y., Lesbani, A. (2025). Biohybrid ZnCr-LDH/Spirogyra algae composite for selective adsorption from multi-dye anionic mixtures: Toward enhanced removal of direct yellow. *Next Materials*, 9, 101094. DOI: 10.1016/j.nxmate.2025.101094.

[28] Ahmad, N., Wijaya, A., Arsyad, F.S., Royani, I., Lesbani, A. (2024). Layered double hydroxide-functionalized humic acid and magnetite by hydrothermal synthesis for optimized adsorption of malachite green. *Kuwait Journal of Science*, 51(2), 100206. DOI: 10.1016/j.kjs.2024.100206.

[29] Mohammed, A.A., Hammood, Z.A. (2025). Efficient removal of sulfamethoxazole antibiotic from aqueous solution using red mud/layered double hydroxide nanocomposite: Optimization, kinetic, and isotherm studies. *Results in Surfaces and Interfaces*, 19, 100534. DOI: 10.1016/j.rsurfi.2025.100534.

[30] Sayeri, R., Arsyad, F., Mardiyanto, Fithri, N., Hanifar, Y., Lesbani, A. (2025). Removal of ceftriaxone using modified layered double hydroxide MgAl-LDH with Hylocereus costaricensis extract. *Chimica Techno Acta*, 12(3), 1–10. DOI: 10.15826/chimtech.2025.12.3.07.

[31] Jefri, J., Fithri, N.A., Lesbani, A. (2024). Enhanced Removal Efficiency of Malachite Green Dye Using Gambir Leaf Extract-Modified NiFe LDH Composites: A Study of Cationic Dye Adsorption. *Bulletin of Chemical Reaction Engineering & Catalysis*, 19(4), 573–584. DOI: 10.9767/bcrec.20215.

[32] Bagherzadeh, M., Salehi, G., Rabiee, N. (2024). Rapid and efficient removal of methylene blue dye from aqueous solutions using extract-modified Zn–Al LDH. *Chemosphere*, 350, 141011. DOI: 10.1016/j.chemosphere.2023.141011.

[33] Sebeia, N., Jabli, M., Ghith, A., Saleh, T.A. (2020). Eco-friendly synthesis of Cynomorium coccineum extract for controlled production of copper nanoparticles for sorption of methylene blue dye. *Arabian Journal of Chemistry*, 13(2), 4263–4274. DOI: 10.1016/j.arabjc.2019.07.007.

[34] Altaf, S., Zafar, R., Zaman, W.Q., Ahmad, S., Yaqoob, K., Syed, A., Khan, A.J., Bilal, M., Arshad, M. (2021). Removal of levofloxacin from aqueous solution by green synthesized magnetite (Fe3O4) nanoparticles using Moringa olifera: Kinetics and reaction mechanism analysis. *Ecotoxicology and Environmental Safety*, 226, 112826. DOI: 10.1016/j.ecoenv.2021.112826.

[35] Ávila-Avilés, R.D., Martínez-Montero, J.P., Villanueva-López, M.A., Ruiz-Ruiz, V.F., Vilchis-Nestor, A.R. (2025). Sustainable bioreduction of graphene oxide via isopropanol-based Camellia sinensis extracts: Influence of tea varieties. *Solid State Communications*, 403, 115995. DOI: 10.1016/j.ssc.2025.115995.

[36] Manimehala, U., Asha, S., Tomy, M., Anu, M.A., Sumitha, M.S., Kumar, P., Xavier, T.S., Binoy, J. (2025). Green synthesis of copper oxide nanoparticles from Camellia sinensis extract: Effects of calcination temperatures on antimicrobial activity. *Biochemical and Biophysical Research Communications*, 769, 151963. DOI: 10.1016/j.bbrc.2025.151963.

[37] Genovese, S., Epifano, F., Marchetti, L., Bastianini, M., Cardellini, F., Spogli, R., Fiorito, S. (2021). Pre-concentration of active principles from different varieties of Camellia sinensis extracts by solid sorbents. *Journal of Pharmaceutical and Biomedical Analysis*, 196, 113945. DOI: 10.1016/j.jpba.2021.113945.

[38] Lesbani, A., Ahmad, N., Mohadi, R., Royani, I., Wibiyan, S. (2024). Selective adsorption of cationic dyes by layered double hydroxide with assist algae (Spirulina platensis) to enrich functional groups. *JCIS Open*, 15(June), 100118. DOI: 10.1016/j.jciso.2024.100118.

[39] Han, J.H., Keum, D.H., Kothuri, V., Kim, Y.J., Kwon, H.C., Kim, D.H., Jung, H.S., Han, S.G. (2024). Enhancing emulsion, texture, rheological and sensory properties of plant-based meat analogs with green tea extracts. *Food Chemistry: X*, 24(June), 101807. DOI: 10.1016/j.fochx.2024.101807.

[40] Luo, Y., Wang, Y., Hua, F., Xue, M., Xie, X., Xie, Y., Yu, S., Zhang, L., Yin, Z., Xie, C., Hong, Z. (2023). Adsorption and photodegradation of reactive red 120 with nickel-iron-layered double hydroxide/biochar composites. *Journal of Hazardous Materials*, 443(PB), 130300. DOI: 10.1016/j.jhazmat.2022.130300.

[41] Zakaria, S.A., Ahmadi, S.H., Amini, M.H. (2024). Investigation the AMOST effect on the sensitivity of CeO2/Ni-Al layered double hydroxide composite based sensors. *Microchemical Journal*, 207, 112128. DOI: 10.1016/j.microc.2024.112128.

[42] Hezari, S., Olad, A., Dilmaghani, A. (2022). Modified gelatin/iron- based metal-organic framework nanocomposite hydrogel as wound dressing: Synthesis, antibacterial activity, and Camellia sinensis release. *International Journal of Biological Macromolecules*, 218(July), 488–505. DOI: 10.1016/j.ijbiomac.2022.07.150.

[43] Jefri, J., Fithri, N.A., Ramadhan, N. (2025). Enhanced Selectivity of Ni/Al LDH for Cationic Dye Adsorption via Gambier Leaf Extract Modification. *Indonesian Journal of Material Research*, 3(1), 1–7. DOI: 10.26554/ijmr.20253148.

[44] Ahmad, N., Marlan, A.R., Negara, S.P.J. (2024). Insight of Anionic Dyes Adsorption from Their Aqueous Solutions onto MgAl LDH/Lignin: Characterization and Isotherm Studies. *Indonesian Journal of Material Research*, 2(2), 40–46. DOI: 10.26554/ijmr.20242233.

[45] Normah, N., Oktriyanti, M., Badri, A.F. (2024). Effectiveness of Modified ZnAl-LDH Developed with POM for Competitive Adsorption of Heavy Metals in Purification Systems. *Indonesian Journal of Material Research*, 2(3), 93–100. DOI: 10.26554/ijmr.20242347.

[46] Lesbani, A., Ahmad, N., Wibiyan, S., Wijaya, A., Amri, Hanifah, Y., Royani, I., Mohadi, R. (2025). Improving congo red dye removal by modification layered double hydroxide with microalgae and macroalgae: Characterization and parametric optimation. *Colloids and Surfaces A: Physicochemical and Engineering Aspects*, 706, 135770. DOI: 10.1016/j.colsurfa.2024.135770.

[47] Badri, A.F., Siregar, P.M.S.B.N., Palapa, N.R., Mohadi, R., Mardiyanto, M., Lesbani, A. (2021). Mg-Al/Biochar Composite with Stable Structure for Malachite Green Adsorption from Aqueous Solutions. *Bulletin of Chemical Reaction Engineering & Catalysis*, 16(1), 149–160. DOI: 10.9767/bcrec.16.1.10270.149-160.

[48] Bisht, K., Pandey, N., Gautam, S., Lohani, P. (2024). Determination of Polyphenols, Reducing Potential and FT-IR Analysis of Green Tea (Camellia sinensis L.) Leaves Extract for Nanoparticles Synthesis. *Journal of Advances in Biology & Biotechnology*, 27(8), 842–850. DOI: 10.9734/jabb/2024/v27i81206.

[49] Li, H., Zhang, Z., Chen, J., Sun, M., Tang, H. (2025). Effect of Cu2+ on the binding of catechins to zein through multi-spectral and in silico analyses. *Food Chemistry*, 463, 141547. DOI: 10.1016/j.foodchem.2024.141547.

[50] Bijlsma, J., de Bruijn, W.J.C., Velikov, K.P., Vincken, J.-P. (2022). Unravelling discolouration caused by iron-flavonoid interactions: Complexation, oxidation, and formation of networks. *Food Chemistry*, 370, 131292. DOI: 10.1016/j.foodchem.2021.131292.

[51] Palapa, N.R., Putra, M.B.K., Musifa, E., Yuliasari, N., Adawiyah, R. (2024). Preparation and Application of Biochar from Areca catechu L. Peel for Malachite Green and Reactive Blue Dyes Removal. *Indonesian Journal of Environmental Management and Sustainability*, 9(1), 28–35. DOI: 10.26554/ijems.2025.9.1.28-35.

[52] Amri, A., Hanifah, Y. (2023). Synthesis of Graphene Oxide using Hummers Method as Adsorbent of Malachite Green Dye. *Indonesian Journal of Material Research*, 1(1), 29–34. DOI: 10.26554/ijmr.2023113.

[53] Velusamy, S., Roy, A., Sundaram, S., Mallick, T.K. (2022). Employing CdS nanoparticles as an adsorbent for the removal of different dosages of hexavalent Cr(VI) from aqueous solution. *Materials Letters*, 311, 131602. DOI: 10.1016/j.matlet.2021.131602.

[54] Olusegun, S.J., Osial, M., Souza, T.G.F., Krajewski, M., Rodrigues, G.L.S., Marek, P., Krysinski, P. (2023). Comparative characteristics and enhanced removal of tetracycline and ceftriaxone by Fe3O4-lignin and Fe3O4-carbon-based lignin: Mechanism, thermodynamic evaluation, and DFT calculation. *Journal of Molecular Liquids*, 371, 121075. DOI: 10.1016/j.molliq.2022.121075.

[55] Yegane Badi, M., Azari, A., Pasalari, H., Esrafili, A., Farzadkia, M. (2018). Modification of activated carbon with magnetic Fe 3 O 4 nanoparticle composite for removal of ceftriaxone from aquatic solutions. *Journal of Molecular Liquids*, 261, 146–154. DOI: 10.1016/j.molliq.2018.04.019.

[56] Madiseh, E.S., Hallajian, S., Faraji, A.R., Zebardast, T., Youseftabar-Miri, L. (2025). Chitosan/Plantago major L. seed mucilage hydrogels incorporated with green synthesized CeO2 nanoparticles for targeted delivery of ceftriaxone: Synthesis, characterization, kinetics, and in vitro cytotoxicity evaluation studies. *Inorganic Chemistry Communications*, 180, 114892. DOI: 10.1016/j.inoche.2025.114892.

[57] Padmavathy, K.S., Madhu, G., Haseena, P.V. (2016). A study on Effects of pH, Adsorbent Dosage, Time, Initial Concentration and Adsorption Isotherm Study for the Removal of Hexavalent Chromium (Cr (VI)) from Wastewater by Magnetite Nanoparticles. *Procedia Technology*, 24, 585–594. DOI: 10.1016/j.protcy.2016.05.127.

[58] Adawiyah, R., Yuliasari, N., Hanifah, Y., Alawiyah, K., Rahayu Palapa, N. (2024). Utilizing Areca catechu L. Fruit Peel-Derived Biochar and Hydrochar for Congo Red Adsorption: Kinetic and Thermodynamic Analysis. *Indonesian Journal of Environmental Management and Sustainability*, 8(4), 135–144. DOI: 10.26554/ijems.2024.8.4.135-144.

[59] Wijaya, A., Ahmad, N., Hanum, L., Melwita, E., Lesbani, A. (2025). Spirogyra sp. macro-algae-supported NiCr-LDH adsorbent for enhanced remazol red dye removal. *Results in Surfaces and Interfaces*, 18, 100427. DOI: 10.1016/j.rsurfi.2025.100427.

[60] Milanković, V., Tasić, T., Brković, S., Potkonjak, N., Unterweger, C., Pašti, I., Lazarević-Pašti, T. (2025). Sustainable carbon materials from biowaste for the removal of organophosphorus pesticides, dyes, and antibiotics. *Journal of Environmental Management*, 376, 124463. DOI: 10.1016/j.jenvman.2025.124463.

[61] Alsuhaibani, A.M., Refat, M.S., Adam, A.M.A., El-Desouky, M.G., El-Bindary, A.A. (2023). Enhanced adsorption of ceftriaxone antibiotics from water by mesoporous copper oxide nanosphere. *Desalination and Water Treatment*, 281, 234–248. DOI: 10.5004/dwt.2023.29135.

[62] Shi, X., Karachi, A., Hosseini, M., Yazd, M.S., Kamyab, H., Ebrahimi, M., Parsaee, Z. (2020). Ultrasound wave assisted removal of Ceftriaxone sodium in aqueous media with novel nano composite g-C3N4/MWCNT/Bi2WO6 based on CCD-RSM model. *Ultrasonics Sonochemistry*, 68, 104460. DOI: 10.1016/j.ultsonch.2019.01.018.

[63] Rinawati, Rahmawati, A., Muthia, D.R., Imelda, M.D., Latief, F.H., Mohamad, S., Kiswandono, A.A. (2024). Removal of ceftriaxone and ciprofloxacin antibiotics from aqueous solutions using graphene oxide derived from corn cob. *Global Journal of Environmental Science and Management*, 10(2), 573–588. DOI: 10.22035/gjesm.2024.02.10.

[64] Bozorginia, S., Jaafari, J., Taghavi, K., Ashrafi, S.D., Roohbakhsh, E., Naghipour, D. (2023). Biosorption of ceftriaxone antibiotic by Pseudomonas putida from aqueous solutions. *International Journal of Environmental Analytical Chemistry*, 103(9), 2067–2081. DOI: 10.1080/03067319.2021.1887858.

[65] Amri, A., Wibiyan, S., Wijaya, A., Ahmad, N., Mohadi, R., Lesbani, A. (2024). Efficient Adsorption of Methylene Blue Dye Using Ni/Al Layered Double Hydroxide-Graphene Oxide Composite. *Bulletin of Chemical Reaction Engineering & Catalysis*, 19(2), 181–189. DOI: 10.9767/bcrec.20121.